Elimination of the endocrine disruptor diethyl phthalate (DEP) using porous materials in advanced oxidative processes (AOP)

Maria Carolina de Almeida[a,*], Tatianne Ferreira de Oliveira[a],
Fernando Pereira de Sá Pereira[b]

[a]*School of Agronomy, Federal University of Goiás- UFG, Km-0, Caixa Postal 131, CEP 74690-900, Goiânia, Brazil,
emails: almeida_mca@hotmail.com (M.C. de Almeida), ferreira.tatianne@yahoo.com.br (T.F. de Oliveira)*
[b]*Federal Institute of Education, Science and Technology of Goiás - IFG, Vale das Goiabeiras, CEP 75400-000, Inhumas, Brazil,
email: fernandofpsa@gmail.com*

ABSTRACT

The object of this study was to evaluate different methods of elimination of the micro-pollutant diethyl phthalate (DEP), within an advanced oxidative process – UV-C/H_2O_2 – and coupling with activated carbon (UV-C/H_2O_2/AC), by comparing the kinetics of each process at constant levels. This study of the kinetics of adsorption and oxidation followed a factorial design of eleven tests, varying the pH's of the medium, temperature and H_2O_2 concentration. The experimental conditions with the highest results were found in tests K9, K10 and K11, which presented a DEP elimination rate of approximately 95.82%; 98.41% and 96.90%, respectively, at pH 7, using 20 mM of H_2O_2 at 30°C for 60 min. For the elimination rate of the pollutant DEP (%), the pH variable showed a significant variance of ($p < 0.05$). The study of the contribution in heterogeneous and homogeneous phases revealed a higher percentage for homogeneous phase efficacy; however, there was AC catalytic activity determined by the application of the radical inhibitor (t-butanol). The thermo-gravimetric analysis of the AC determined the mass of the adsorbed products in the AC, whereas scanning electron microscopy analysis revealed the possibility of AC reuse, because the textural properties were maintained. Therefore, the UV-C/H_2O_2/AC coupling process proposed in the treatment of DEP elimination in effluent is efficient and is an alternative for the degradation of this micro-pollutant in aqueous phases.

Keywords: Diethyl phthalate; Advanced oxidative process; UV-C/H_2O_2, UV-C/H_2O_2/AC coupling

1. Introduction

The adoption of a greater rigor in wastewater disposal standards has motivated research and, in tandem, has shown a need for greater technological development towards reducing its environmental impact, especially in effluents containing high levels of micro-pollutants, such as those from, among others, the food and pharmaceutical industries. In the countries of the European Union, the preservation of water quality and consequently of aquatic environments is a priority that has led to an evolution in legislation. As an example, Directive Cadre sur l'eau (DCE) 2000/60/EC of 23rd October 2000 (Framework for Water) provides for a 30% reduction by 2021, of several substances classified as priority because of their hazardous nature when present in industrial effluents [1].

Among these micro-pollutants are phthalates, phthalic acid esters and a group of chemicals that cause serious environmental concerns due to their potential eco-toxicological risk [2–4]. The use of phthalates is mainly found when used as plastic additives, especially in plasticized polyvinyl chloride (PVC), as well as in the production of paints and varnishes, adhesives, lubricants and cosmetics [5].

* Corresponding author.

Phthalates are known to be chemicals hazardous for human health as they have been associated with birth defects, organ damage, infertility and cancer. They are also known to be among the endocrine disrupting compounds present in water [6], and have been shown to be acutely toxic in animal and human samples, but chronic studies, especially with rodents have shown reproductive toxicity [7–11].

Several studies have quantified endocrine disrupters in industrial, domestic and even treated water discharges, that is, water to be distributed for human consumption, and which demonstrate the inefficiency of the currently installed processes [12]. Another point is the increased need for reuse of some environmental assets, such as water, which requires improvements in sewage and effluent treatment systems. So specific treatment processes need to be implemented as the sources of emerging contaminants cannot be eliminated in their entirety.

In this context, advanced oxidative processes (AOPs) have been studied and are considered an alternative tertiary treatment for hazardous and/or toxic micro-pollutants, based on the formation of radical reactive hydroxyl (HO•) species. In addition, the use of organic solvents in the treatment of organic and inorganic pollutants has been reported in the literature [13–17]. Some studies have shown that a hybrid process which combines high oxidation capacity and the use of materials acting as radical initiators (HO•), that is, those that promote oxidation instead of acting as an adsorbent, such as activated carbons, iron oxides, titania and alumina [18]. These can be very efficient systems when compared with conventional AOP [19], and is one of the perspectives and recommendations for AOP's in the future [20].

The objective of this work was to use porous materials such as AC, combined with AOP to eliminate diethyl phthalate (DEP), determining the kinetic constants by the AOP treatments (UV-C/H_2O_2) and coupling using AC (UV-C/H_2O_2/AC), as well as the contribution of both homogeneous and heterogeneous phases in the elimination of this micro-pollutant.

2. Materials and methods

2.1. Materials and activated carbon characterization

Activated carbon was donated by FBC (Fábrica Brasileira de Catalisadores, Brazil). Textural analysis was performed on a porosimeter (brand Micromeritics, model Gemini V2380). The specific surface area ($m^2\,g^{-1}$) was measured using the BET method (Brunauer, Emmet and Teller). Total pore volume ($cm^3\,g^{-1}$), micro-pore volume ($cm^3\,g^{-1}$), size distribution and average pore diameter (Å) were estimated from the linear part of the Dubinin-Radushkevich plot [21,22]. The Boehm method was used to determine the surface functional groups (acidic and basic) [23]. The determination of the point of zero charge (pH_{PZC}) was carried out using the method proposed by Regalbuto and Robles [24]. Adsorption spectra in the infrared region, Fourier transform infrared spectroscopy (FTIR), was obtained using a spectrophotometer (brand PerkinElmer, model Spectrum 400). The analyses were concentrated in the infrared region between 4,000 and 400 cm^{-1}, with a resolution of 4 cm^{-1}. Scanning electron microscopy (SEM) analyses were performed using an electron scanning electron microscope (brand JEOL, model JSM - 6610), with the aim of evaluating the morphology of activated carbon.

DEP of the brand Aldrich Chemistry showed 99.5% purity. All chemicals used were of analytical grade.

2.2. Thermo-gravimetric analysis

Pre-kinetic and post-kinetic AC analyses were performed according to Ramos et al. [32] in a thermo-mechanical analyzer (brand Shimadzu TMA50, model DTG 60/60H) coupled with a differential scanning calorimeter (model 60 PLUS). Samples were placed in an oven at 80°C for 24 h prior to each thermo-gravimetric analysis (TGA). The 0.2 g mass of AC was introduced into platinum crucibles at a synthetic air flow rate of 10 L min^{-1} up to a temperature of 1,200°C. Samples were heated at a rate of 10°C min^{-1}.

2.3. Scanning electron microscopy

The morphological characteristics of the pre-kinetic AC and post-kinetic coupling were performed according to Zhang et al. [25], using a JEOL, JSM – 6610 model, Tokyo, Japan, equipped with an energy scattering spectrometer (Thermo scientific brand NSS spectral imaging in a scanning electron microscope (MEV).

2.4. H_2O_2/UV-C and H_2O_2/UV-C/activated carbon coupling

The oxidation kinetics was performed as follows: varying the H_2O_2 concentration which was added to a photo-reactor containing 250 mL of the effluent to a 0.2 g L^{-1} concentration of the micro-solvent DEP, (which was chosen as the standard). Experimentation started when H_2O_2 was introduced into the photo-reactor. The photo-reactor consisted of a parabolic glass cell containing the micro-pollutant solution which was placed under a 125 W mercury vapor lamp bulb (brand AVANT) with a 20.41 W m^2 light intensity (UV-C). This system was placed on a magnetic stirrer (NOVA TÉCNICA brand) with agitation control set at 150 rpm at a given temperature according to the experimental design. Three variables were studied (Table 1): the concentration of H_2O_2 introduced into the photo-reactor (10; 20; 30 mM), the pH of the solution (3; 7; 11) and the temperature (15°C; 30°C; 45°C). In AC coupling, the same experimental procedure was followed; with the addition of 0.4 g of AC (preliminary tests which are not presented in this work were completed to choose the AC mass).

During the oxidation processes, samples were collected at different time intervals (0, 12, 24, 36, 48, 60, 80, 100, 120 min) to evaluate the elimination of the pollutant in the solution. 2 mL of aliquot were collected at these time intervals, and 1 mL of sodium sulphite (Na_2SO_3) at 0.1 M L^{-1} was added as an HO• radical inhibitor, according to the methodology proposed by Liu et al. [26]. The samples were conditioned in test tubes wrapped in foil, thereby eliminating the possibility of light degradation after collection right up to the moment of analysis.

Table 1
Influencing factors investigated

Factors	Code	–1	0	1
H_2O_2 (mM)	x_1	10	20	30
pH	x_2	3	7	11
Temperature	x_3	15	30	45

Analyzes of the DEP concentration of the processes under study were performed using high performance liquid chromatography. The chromatographic system used was fitted with the following brands of equipment: SCHIMADZU C202047; model LC-8A; detector: UV/VIS PROMINENCE SPD-20A DAD (λ = 228 nm); column: C18 (250 mm × 4.6 mm × 5 μm), WAKOSIL brand, model SGE 206505, mobile phase: acetonitrile (ACN P.A.)/water (Milli-Q deionized H_2O) 70:30; flow of the mobile phase: 1 mL s^{-1}; limit of instrumental detection: 0.12–0.17 μg L^{-1} for DEP; sample injection volume: 20 μL.

The readings of the DEP concentrations were determined by the area of the chromatographic peak obtained after 7 continuous minutes. The percentage of elimination of DEP (%) was calculated using Eq. (1):

$$ta_t = \frac{\left[DEP\right]_0 - \left[DEP\right]_t}{\left[DEP\right]_0} . 100 \tag{1}$$

where $[DEP]_0$ and $[DEP]_t$ = concentrations of DEP, respectively, at the initial time and at time t (g L^{-1}); ta$_t$ = rate of elimination of DEP (%) over time.

2.4.1. H₂O₂/UV-C/activated carbon/tert-butanol coupling

Oxidation kinetics with the presence of the hydroxyl radical inhibitor (HO•) (t-BuOH), were completed using the same previous experimental protocol, but with the addition of 60 mM of t-BuOH in a stoichiometric proportion to slow and inhibit the production of hydroxyl radicals (HO•), according to methodology proposed by Oliveira et al. [27] and Acosta [28].

2.4.2. Kinetic model of treatments H₂O₂/UV-C, H₂O₂/UV-C/AC and H₂O₂/UV-C/AC/tert-butanol

A kinetic model was proposed to describe the oxidation kinetics of DEP by AOP, which was a first-order homogeneous phase (without AC) [5,17,29], determining the oxidation rate constant of DEP (homogeneous). In the heterogeneous phase (with AC), that is, H_2O_2/UV-C/AC, we were able to calculate the global velocity constant (k_{global}), according to the following equations:

The direct or indirect degradation of DEP can be expressed by the following equation:

$$-\ln \frac{[DEP]_{final}}{[DEP]_{initial}} = k_{homogeneous} . t \tag{2}$$

Thus, $k_{homogeneous}$ is the slope of Eq. (2) and represents the first-order kinetic constant for the reaction rate in a solution of H_2O_2/UV-C (in the absence of activated carbon).

k_{global} represents the global reaction constant in the heterogeneous phase (in the presence of activated carbon) and homogeneous phase (Eq. (3)):

$$-\ln \frac{[DEPl]_{final}}{[DEP]_{initial}} = k_{global} . t \tag{3}$$

The determination of k_{global} allowed us to calculate the kinetic constant of the heterogeneous reaction ($k_{heterogeneous}$) (Eq. (6)), $\delta_{homogeneous}$ and $\delta_{heterogeneous}$ according to Eqs. (4)–(6):

$$k_{global} = k_{homogeneous} + k_{heterogeneous} \tag{4}$$

$$\delta_{homogeneous} = \frac{k_{homogeneous}}{k_{global}} . 100 \tag{5}$$

$$\delta_{heterogeneous} = \frac{k_{heterogeneous}}{k_{global}} . 100 \tag{6}$$

For the experiments with H_2O_2/UV-C/AC/tert-butanol, the radical reactions were eliminated and the equation can be simplified as:

$$-\ln \frac{[DEP]_{final}}{[DEP]_{initial}} = k_{globalobs} . t \tag{7}$$

With the determination of k_{global} and $k_{global\,obs}$ through Eqs. (3) and (7), respectively, it was possible to estimate the kinetic contribution of the radical reactions in the degradation of DEP ($\delta_{HO}°$), according to Eq. (8):

$$\delta_{OH°} = \frac{k_{global} - k_{globalobs}}{k_{global}} . 100 \tag{8}$$

The data obtained were analyzed using Statistica 7.0 (StatSoft Inc., Tulsa, Oklahoma, United States), with a significance level of ($p < 0.05$), to determine the response surfaces. The criterion for choosing the best adjustments was based on the determination coefficient (R^2).

3. Results and discussion

3.1. Activated carbon characterization

The results of the chemical characterization of AC used in this study are presented in Table 2, and show that this AC has a predominantly basic character, but it changes, however,

Table 2
Chemical characteristics of oxygenated groups on the surface of AC

pH$_{PZC}$	Carboxylics (meq g^{-1})	Phenolics (meq g^{-1})	Lactones (meq g^{-1})	Total acid (meq g^{-1})	Total basic (meq g^{-1})[a]	FTIR (cm^{-1})
7.2	0.071	0.169	0.211	0.523	0.845	1,500–1,800

according to the nature of different acid groups: 15.09% carboxylic acids; 36.36% phenolic and 47.72% lactones. The obtained pH_{PZC} was consistent with the quantification of surface functional groups obtained using the Boehm method and had a pH value of 7.2. The result obtained by infrared analysis is consistent when compared with the Boehm method and pH_{PZC}, where the adsorption wavelength for (A) phenol acid was identified (Fig. 1); (B) carboxylic acid, anhydride and lactone and (C) carbonyl and quinone groups, respectively [30,31]. The FTIR analysis indicated a higher carbonaceous content (75.3% C, 0.6% H, 0.5% N and 10.4% O), being in concordance with the AC from an agro-industrial by-product [32]. The textural characterization (Table 3) indicates that the
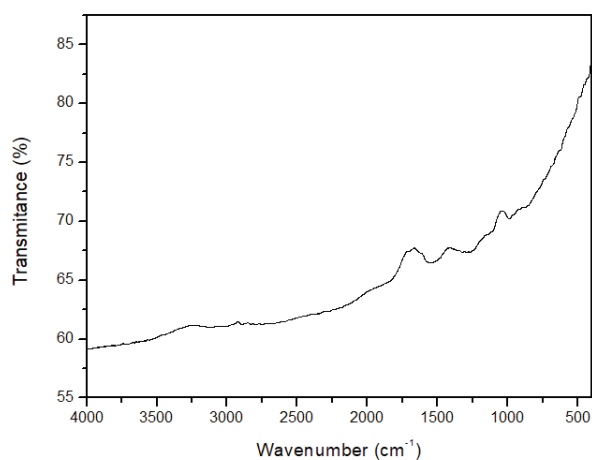

Fig. 1. Spectrum in the infrared region (FTIR) of crude activated carbon.

AC has a high S_{micro}, being mainly composed of micropores with radius of 0.160 to 0.263.

3.2. DEP kinetic degradation

3.2.1. UV-C/H_2O_2

The kinetic curves of the AOP in the elimination of DEP were modelled to determine the $k_{homogeneous}$ and the results obtained are presented in Table 4.

The coefficients of determination (R^2) obtained in the 11 experiments allowed us to conclude that the model is satisfactory for the obtained data, where $R^2 \geq 0.984$, and where the highest $k_{homogeneous}$ values were obtained in the experiments at pH 3 and 7. An example of this is seen in the $k_{homogeneous}$ of 0.407 min^{-1} at K11 (pH 7) and 0.0459 min^{-1} at K2 (pH 3), confirming that there is a greater impact of pH on the treatment compared with the H_2O_2 concentration variable and the temperature. However, it has been observed that $k_{homogeneous}$ is linearly dependent on the concentration of H_2O_2, since the concentration of the HO• radicals increases when the initial concentration of H_2O_2 is increased [5,33].

Studies performed with AOP UV/H_2O_2 to eliminate phthalates also returned positive results. According to Xu et al. [33], DEP elimination of more than 98.6% was observed in 60 min, in a concentration of 20 mg L^{-1} of H_2O_2; with an increase of H_2O_2 (2.5–30 mg L^{-1}) served to increase the removal efficiency by 16.8%–99.8%; while the intensity of UV radiation increased the efficiency of DEP removal due to the production of more hydroxyl radicals. Xu et al. [34] studied AOP in the elimination of dimethyl phthalate (DMP), but the results verified that direct oxidation with H_2O_2 does not oxidize the DMP molecule in a reaction period of 3 h. The first-order rate constant increases with increasing

Table 3
Textural features of AC

Area single point $(p/p0 = 0.29)$ (m^2 g^{-1})	Micropore radius (Å) BJH method	W_0 (cm^3 g^{-1})	L_0 (Å)	S_{BET} (m^2 g^{-1}) BET method	S_{ext} (m^2 g^{-1})	S_{micro} (m^2 g^{-1})	S_{total} (m^2 g^{-1})
596.946	0.16–0.263	0.253	20.796	554.228	94.174	460.054	554.228

Table 4
Kinetic parameters of the first order model applied to AOP treatment for elimination of DEP

		First-order model			
Kinetics of AOP	[H_2O_2] (mM)	pH	Temperature (°C)	$k_{homogeneous}$ (min^{-1})	R_1^2
K1	10	3	15	0.0251	0.9958
K2	30	3	15	0.0459	0.9878
K3	10	11	15	0.0055	0.9881
K4	30	11	15	0.0079	0.9909
K5	10	3	45	0.0205	0.984
K6	30	3	45	0.0509	0.9981
K7	10	11	45	0.0037	0.9783
K8	30	11	45	0.0099	0.9803
K9	20	7	30	0.0430	0.997
K10	20	7	30	0.0390	0.9926
K11	20	7	30	0.0407	0.9965

initial H_2O_2 concentration (2.5–40 mg L^{-1}), however, a higher concentration causes the elimination of HO• radicals; and the degradation of DMP decreases with increasing concentration in an exponential trend. It was also confirmed that the first-order rate constant increased according to an increasing pH (2.5–4) but decreased at higher pH levels.

3.2.2. UV-C/H_2O_2/AC

The curves of DEP oxidation kinetics by UV-C/H_2O_2/AC coupling are shown in Fig. 2. The results show that the higher rates of DEP elimination by the AOP and AC coupling, and the shorter times required for photo-oxidation of DEP (pH 3, 10 mM of H_2O_2, 15°C), are 99.62% after 120 min and at K10 (pH 7, 20 mM of H_2O_2, 30°C); 98.41% after 60 min. However, less time was required for photo-oxidation of K6 (pH 3, 30 mM of H_2O_2, 45°C), at 80 min, with a rate of 98.22%. The K7 kinetics at pH 11, 10 mM H_2O_2, 45°C, 0.4 g AC showed the lowest DEP elimination rate by the 35.14% coupling and it was unable to eliminate the DEP micro-pollutant in less than 120 min.
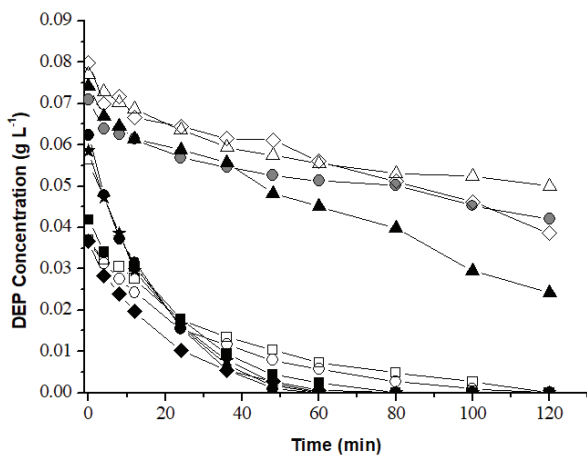

Fig. 2. Kinetic curves of the oxidation coupling and DEP adsorption are obtained by plotting the DEP concentration (g L^{-1}) as a function of time (min) of K1 (○) pH 3, 10 mM H_2O_2, 15°C; K2 (■) pH 3, 30 mM H_2O_2, 15°C; K3 (●) pH 11, 10 mM H_2O_2, 15°C; K4 (◇) pH 11, 30 mM H_2O_2, 15°C; K5 (□) pH 3, 10 mM H_2O_2, 45°C; K6 (◆) pH 3, 30 mM H_2O_2, 45°C; K7 (△) pH 11, 10 mM H_2O_2, 45°C; K8 (▲) pH 11, 30 mM H_2O_2, 45°C; K9 (*) pH 7, 20 mM H_2O_2, 30°C; K10 (●) pH 7, 20 mM H_2O_2, 30°C; K11 (-) pH 7, 20 mM H_2O_2, 30°C.

These results show that there were interactions between the DEP at alkaline pH and the coupling so that pH was more influential for DEP degradation than other variables such as H_2O_2 concentration and temperature. This was confirmed, when we found that K8, a test at pH 11, 30 mM H_2O_2, 45°C, showed a DEP elimination rate (%) of 67.28%. Thus, it was noted that at the same temperature, the H_2O_2 concentration was more important in degradation than the temperature itself.

The regression coefficients presented in Table 5 were calculated from the kinetic results obtained. The regression coefficients were significant at a level of 5% ($p < 0.05$) for pH ($p = 0.021441$). It was also evidenced in the Pareto diagram of the standardized effects presented in Fig. 3.

The average points presented small variations for the rates of elimination of DEP by AOP and AC, in the kinetics K9, K10 and K11, varying between 95.82; 98.41 and 96.90%, respectively. DEP elimination time by coupling was 60 minutes, thereby demonstrating a possibility of repeating the treatment condition (standard deviation less than 5%).

The response surfaces presented in Fig. 4 also showed higher values of DEP elimination rate by the couplings with the lower pH but higher values of the H_2O_2 concentration. The effect of this variable is positive, that is, when there is an increase in H_2O_2 concentration, there is an increase in the rate of elimination of DEP by the coupling. The pH, however,
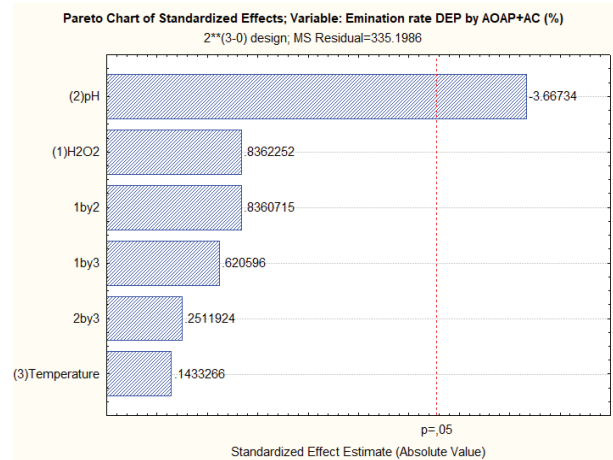

Fig. 3. Pareto diagram of the standardized effects for Y_1 response (DEP elimination rate (%) by coupling).

Table 5
Regression coefficients for Y_1 response (rate of elimination of DEP by UV-C / H_2O_2 / AC coupling).

| Factors	Regression coefficients	Standard error	t(4)	p value	Ranges estimates (95%)	
					Lower limit	Higher limit
Mean	79.1155	5.20199	14.33200	0.000138	63.7889	94.44200
(x_1) [H_2O_2]	5.4129	6.473008	0.83623	0.450073	−12.5591	23.38484
(x_2) pH	−23.7387	6.473008	−3.66734	0.021441	−41.7107	−5.76679
(x_3) Temperature	0.9278	6.473008	0.14333	0.892963	−17.0442	18.89970
x_1 e x_2	5.4119	6.473008	0.83607	0.450150	−12.5601	23.38385
x_1 e x_3	4.0171	6.473008	0.62060	0.568477	−13.9548	21.98907
x_2 e x_3	1.6260	6.473008	0.25119	0.814042	−16.3460	19.59792

(a)

(b)

(c)
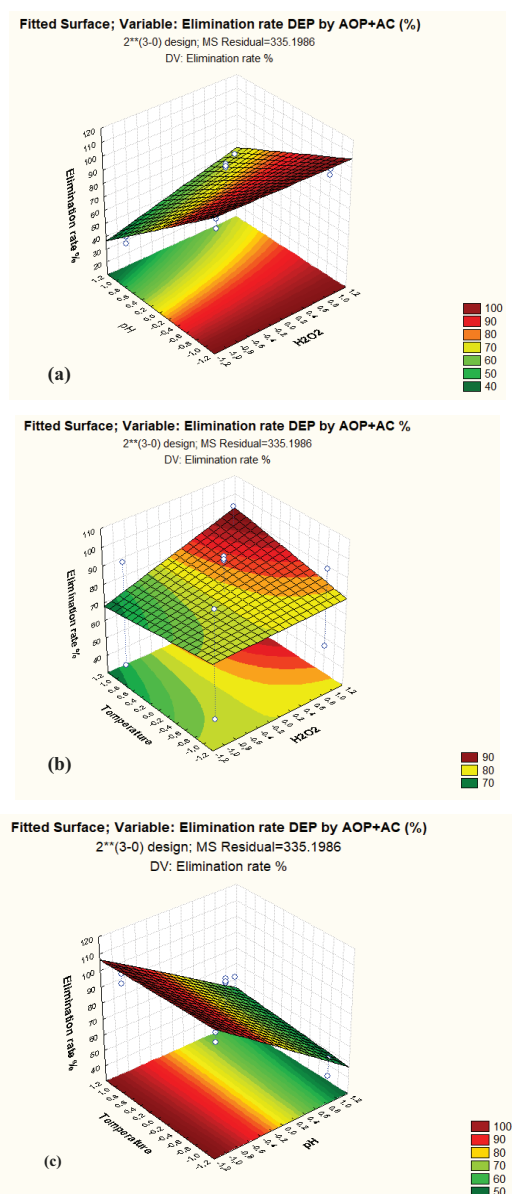
Fig. 4. (a) Response surface for DEP elimination rate (%) by AOP + AC (Y_1) as a function of pH and H_2O_2 concentration (mM); (b) Response surface for DEP elimination rate (%) by AOP + AC (Y_1) as a function of temperature (°C) and H_2O_2 concentration (mM); (c) Response surface for DEP elimination rate (%) by AOP + AC (Y_1) as a function of temperature (°C) and pH.

Fig. 5. Comparison between the kinetics with the highest rates of elimination of DEP, K9 (■) pH 7, 20 mM H_2O_2, 30°C (UV-C/H_2O_2); and K10 (△) pH 7, 20 mM/H_2O_2, 30°C, 0.4 g UV-C/H_2O_2/AC, plotted as the concentration of DEP (g L^{-1}) as a function of time (min).

has a negative effect, the higher the rate of elimination of DEP, the lower the pH. The temperature between the studied variables has, therefore, a positive effect, but the impact was smaller in comparison with the other variables.

These results also showed that the AC added to the reaction medium in the UV-C/H_2O_2/AC process resulted in reduced pH for DEP elimination compared with the non-AC applied AOP treatment (Fig. 5). Therefore, there is a greater efficacy in the kinetics of pH 7, 20 mM of H_2O_2 30°C, since there was a reduction in time taken from 100 min (AOP) to 60 min with the coupling (AOP and AC). At pH 3, 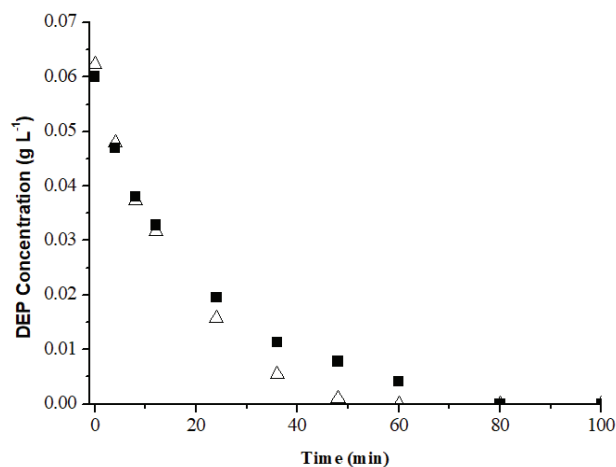the time taken to eliminate DEP was also reduced, from 100 min (AOP) to 80 min (AOP and AC coupling), at K6 (pH 3, 30 mM/H_2O_2, 45°C).

As reported in the literature, some studies using advanced oxidative processes [5,19,27,35], O_3/AC present an attractive option for increasing elimination efficiency, because the presence of AC promotes the generation of HO• radicals. Medellin-Castillo et al., [5], stated that the addition of ACs increased DEP degradation kinetics, where there was 85% and 90% elimination in 20 min, while only 40% was obtained without AC. The authors also explain that the catalytic activity of ACs depends on chemical and texture properties (basicity and area). More detailed studies on the influence of the chemical and texture properties of activated carbon on ozonation of organic compounds were published, and it was verified that basic groups on the surface of activated carbon are the most important characteristic for improving the degradation of pollutants [35]. Thus, activated carbon, with a pH_{PZC} of 10, promoted greater activity for generating HO• than the activated carbon which presented a lower basicity (pH_{PZC} = 6.5).

Studies using 2,4 dichlorophenol (2,4 DCP) micro-pollutants revealed only 15% removal in 90 min, and no mineralization occurred under the experimental condition, 40 mM H_2O_2 at pH 7 and absence of UV-C irradiation; however 91% of 2,4 DCP can be removed by UV-C photolysis in 90 min. The mineralization efficiency at the end of treatment was only 16%, indicating that the use of UV-C treatment alone was not sufficient in the effective degradation of photolysis intermediates 2,4 DCP [17]. Although there are no ionizable functional groups on lindane, H_2O_2 ionizes at higher pH values (pKa = 11.7). The reduction of the reaction rate at pH may reflect a less efficient production of HO• due to the acid-based chemical reaction of H_2O_2 [29]. Thus, for DEP, incomplete mineralization by AOP was also found, as it did not present ionizable functional groups with high pH values, and thus H_2O_2 ionized, producing insufficient HO• for effective treatment. Therefore, from these UV/H_2O_2, UV

and H_2O_2 AOP applied results, it was found that the results of the UV-C/H_2O_2/AC coupling kinetics, the increase of DEP degradation rate in O_3/AC and UV-C/H_2O_2/AC is mainly due to the increase of HO• radicals in the reactor by the presence of AC.

3.2.3. Modelling of the coupling kinetics UV-C/H_2O_2/AC

The values of k_{global} and $k_{heterogeneous}$ were obtained from the data obtained in the oxidation kinetics of DEP by coupling – UV-C/H_2O_2/AC (Table 6), and these were compared with $k_{homogeneous}$ UV-C/H_2O_2.

The coefficients of determination (R^2) obtained for the 11 experiments allow us to conclude that the model is satisfactory for the data obtained, where the highest values of the kinetic constants by the UV-C/H_2O_2/AC process (k_{global}) were determined in the experiments at pH 7 such as, for example, k_{global} of 0.0813 min^{-1} at K10 (pH 7) and lower values at basic conditions with k_{global} of 0.004 min^{-1} at K7 (pH 11). At this stage of the study, among the best performances in terms of degradation kinetics of DEP by UV-C/H_2O_2/AC coupling as well as in the oxidation of DEP by UV-C/H_2O_2, were found in kinetics K9, K10 and K11, all at pH 7 and 30°C. This may confirm that the pH had the greatest impact among the independent variables in relation to the concentration of peroxide (H_2O_2) and the temperature for coupling.

The kinetic results also show that the higher the H_2O_2 concentration, the greater the k_{global} kinetic constant, as evidenced in experiments K1 and K2, both performed at pH 3, 15°C and with k_{global} of 0.0346 min^{-1} in K1 (10 mM of H_2O_2) against k_{global} of 0.0476 min^{-1} in C2 (30 mM of H_2O_2). In the literature, studies have shown that concentration when over-elevated can inhibit the formation of free radicals [36–38]. On the other hand, it can be seen that the pH has a negative aspect, which means that at high pH there is a lower percentage removal of DEP. Brame et al. [39] and Buthiyappan et al. [40] explain that by the deprotonation of H_2O_2 forming HO_2•; the reaction is given by Eq. (9) as follows:

$$H_2O_2 \rightarrow HO_2\bullet \tag{9}$$

As can be seen, H_2O_2 dissociates into HO_2•, which dissociates again into H_2O and O_2, the reaction given by Eq. (10). Thus, the degradation of the peroxide is lower and reduces the yield of free-radical formation kinetics and thus also the percentage of the pollutant removed.

$$H_2O_2 + HO_2\bullet \rightarrow HO\bullet + H_2O + O_2 \tag{10}$$
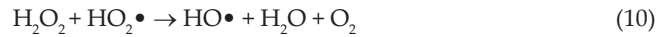
These results confirm that pH is the main factor, and in second place the concentration of H_2O_2, since they remit a positive impact for the percentage removal of DEP during the coupling thereby revealing a better efficiency rate. It can be observed that the ideal factors for coupling were at pH 7 and a H_2O_2 concentration of 20 mM L^{-1}, whereby AOP without AC saw higher rates of DEP elimination presented. Thus, it can be explained by the catalytic effect of AC at higher pH, or near neutrality. This can be confirmed by the repeatability of the results in the factorial design at the central point. The increase in percentage removal at low peroxide concentration may be due to the absorption of the pollutant by AC.

In comparison with the coupling (UV-C/H_2O_2/AC), the same factors have a smaller effect on the removal percentage and have no significant effect on the final concentration as seen with the AOP-free coal experiment. In addition, it can be observed that the pH has a negative effect, assuming a high pH and the external charge of the AC because of the positive charge, and then promote an increase of the catalytic reaction between the AC and H_2O_2 [1,41,42].

The contribution of the oxidation pathway, either homogeneous ($\gamma_{homogeneous}$) or heterogeneous ($\gamma_{heterogeneous}$) is presented in Table 7. The results confirm that the degradation of DEP occurred prior to the homogeneous phase, but a non-negligible part can also occur on the surface of AC, since it accelerated the time of elimination from 100 min, to less than 60 min (with the addition of AC) to the best experimental conditions, K9, K10 and K11, and which is evidenced by Fig. 5. The experimental results are consistent with the literature [43,44], which suggests that the presence of oxygen groups on the sorbent surface of AC, causes an increase in the efficiency of H_2O_2 decomposition and contributes to the generation of hydroxyl radicals.

Table 6
$k_{homogeneous}$, $k_{heterogeneous}$ and k_{global} kinetic parameters applied in the treatment of AOP for elimination of DEP

Kinetics	k_{global} (min^{-1})	R^2	$k_{heterogeneous}$ (min^{-1})	$k_{homogeneos}$ (min^{-1})
K1	0.0346	0.9900	0.0095	0.0251
K2	0.0476	0.9864	0.0017	0.0459
K3	0.0073	0.9415	0.0018	0.0055
K4	0.0107	0.9629	0.0028	0.0079
K5	0.0258	0.9967	0.0053	0.0205
K6	0.0585	0.9894	0.0076	0.0509
K7	0.0040	0.8993	0.0003	0.0037
K8	0.0118	0.973	0.0019	0.0099
K9	0.0634	0.9847	0.0204	0.043
K10	0.0813	0.9627	0.0423	0.039
K11	0.0698	0.9746	0.0291	0.0407

3.2.4. H_2O_2/UV-C/AC/tert-butanol (t-BuOH)

The curves of the kinetics of coupling with hydroxyl radical inhibitor are shown in Fig. 6. According to the results obtained, the differences between the times of elimination of DEP in each treatment can be verified. Especially, the reduction of the time with the addition of AC to the reaction medium was noted. In the comparison between kinetics, the highest elimination rates were considered in each treatment, 99.91% in 100 min of K9 of AOP (UV-C/H_2O_2); 98.41% in 60 min of K10 of the AOP and AC coupling (UV-C/H_2O_2/AC); 99.18% in 120 min of K9 of the radical inhibitor coupling (UV-C/H_2O_2/AC/t-butanol).

These results show that the shortest times required for oxidation and adsorption of DEP were obtained after coupling – requiring only 60 min. The highest times obtained in the coupling with the inhibitor were 120 min, which is twice longer. Coupling with t-butanol reduced the rate of

Table 7
Kinetic contributions $\gamma_{homogeneous}$, $\gamma_{heterogeneous}$

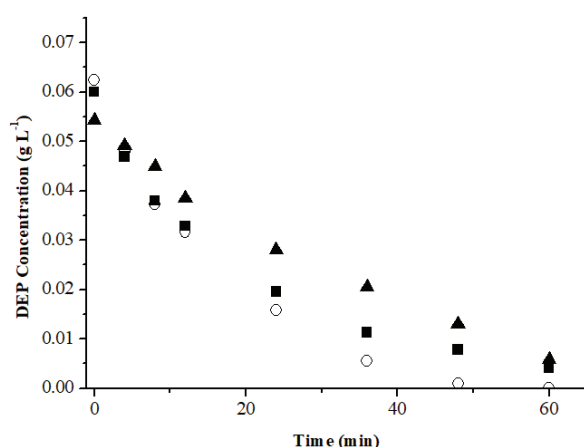| Kinetics	$\gamma_{homogeneous}$ (%)	$\gamma_{heterogeneous}$ (%)
K1	72.543	27.457
K2	96.429	3.571
K3	75.341	24.6585
K4	73.832	26.1682
K5	79.457	20.5436
K6	87.009	12.9915
K7	92.51	7.5
K8	83.988	16.102
K9	67.823	32.177
K10	47.971	52.030
K11	58.309	41.691

Fig. 6. Comparison between the kinetics with the highest rates of elimination of DEP, K9 (■) pH 7, 20 mM H_2O_2, 30°C of AOP; K10 (○) pH 7, 20 mM H_2O_2, 30°C, 0.4 g AC coupling and K9 (▲) (pH 7, 20 mM H_2O_2, 30°C, 0.4 g AC, 60 mM t-butanol (TeOH), plotted as the concentration of DEP (g L⁻¹) as a function of time (min).

elimination of DEP by 50%. In the AOP and AC couplings in 60 min, the DEP elimination rate was 98.41%, while for the radical inhibitor coupling experiments the elimination rate for the experiments with t-BuOH in 120 min was 99.18%.

In the research on DEP elimination by AOPs, couplings and use of radical inhibitors to slow the photo-degradation completed by Medellin-Castillo et al. [5], they also stated that it is very well known that t-BuOH is a hydroxyl radical scavenger, so that it eliminates the contribution of the HO• radicals by lowering the reaction rate. They reported that the kinetics of the direct reaction of DEP with ozone was studied by performing experiments at pH = 7, with and without t-BuOH. The researchers revealed that a percentage degradation of DEP of only 5% was reached in 60 min when t-BuOH was added to the reactor solution. However, the DEP decomposition was considerably improved without t-BuOH because its percentage conversion was 62% in 60 min [45].

Table 8 presents the constant rate with the presence of hydroxyl radicals HO• ($k_{inibidor}$) as well as the contributions of the radical phase $\gamma_{adicalar}$. The results show that the kinetic constants obtained ($k_{inibidor}$) were between 0.0352 and 0.0382 min⁻¹, stating that there was an efficient inhibition of radical formation in the treatment process when compared with the global constants without the presence of t-butanol at pH 7, 30°C and 20 mM of H_2O_2, moving from 0.0634 to 0.0813 min⁻¹. Oliveira et al. [46] also observed that in AOP using O_3/AC there was a decrease in the degradation of the micro-pollutant DEP in the presence of t-BuOH, stating that the degradation is mainly due to radical reactions: based on their high reactivity. The hydroxyl radicals generated are not selective species, and the results obtained in this work are summarized in Table 8 [27,28,47,48].

3.3. AC thermo-gravimetric analysis

The AC's TGA results are shown in Fig. 7(a). It can be observed from the thermal analysis that the first mass slope, between 85°C and 125°C, is due to the loss of moisture, the corresponding value for water desorption (the phenomenon of physisorption) in AC, even after being on the drying ramp prior to TGA. AC decomposition occurs near 625°C. The percentage of residues was approximately 20%. The residues are derived from the oxides formed during the heating process in an oxidizing atmosphere [49]. A greater loss of mass of between 500°C and 625°C of the ACs in the coupling kinetics is observed. For the washed AC, the rate is 17% of the initial mass. This is due to the decomposition characteristics of oxygenated compounds occurring at between 500°C and 800°C,

Table 8
$k_{inibidor}$ kinetic constants (min⁻¹) and $\gamma_{radicalar}$ radical contribution applied to the treatment of AOP + AC + t-BuOH for elimination of DEP

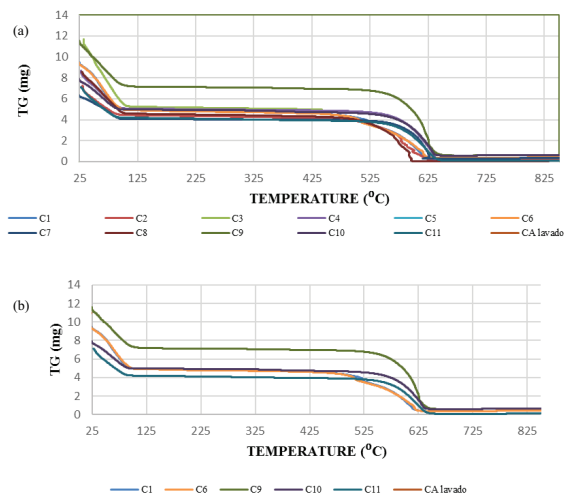| Kinetics	$k_{inibidor}$ (min⁻¹)	R^2	$\gamma_{radicalar}$ (%)	k_{global} (min⁻¹)
K9	0.0352	0.9877	49.1805	0.0634
K10	0.0382	0.9888	38.8565	0.0813
K11	0.0371	0.9916	46.1719	0.0698

Fig. 7. Comparison between thermo-gravimetric analysis (TGA) of DEP saturated AC after the coupling kinetics of AOP and AC, K1 (--) pH 3, 10 mM H_2O_2, 15°C; K2 (--) pH 3, 30 mM H_2O_2, 15°C; K3 (--) pH 11, 10 mM H_2O_2, 15°C; K4 (--) pH 11, 30 mM H_2O_2, 15°C; K5 (--) pH 3, 10 mM H_2O_2, 45°C; K6 (--) pH 3, 30 mM H_2O_2, 45°C; K7 (--) pH 11, 10 mM H_2O_2, 45°C; K8 (--) pH 11, 30 mM H_2O_2, 45°C; K9 (--) pH 7, 20 mM H_2O_2, 30°C; K10 (--) pH 7, 20 mM H_2O_2, 30°C; K11 (--) pH 7, 20 mM H_2O_2, 30°C and the washed (-) AC (pre-kinetic) in an atmosphere of synthetic air.

as reported by Cagnon et al. [50]. Experimental conditions with higher rates of elimination of DEP at pH 3 and pH 7 showed TGA curves as a function of the decomposition of the adsorbed material in AC very similar to each other and also of AC pre-kinetic coupling of AOP and AC, as shown in Fig. 7(b).

3.4. Scanning electron microscopy of the AC

The structure of AC, pre and post the UV-C/H_2O_2/AC process was determined (Fig. 8). The results reveal that pre-use and post-use AC MEV images are still smooth. Some AC particles before use in treatments are difficult to find in the AC MEV images used. However, the AC pore structure was not damaged, assuming that the textural properties had been maintained. Therefore, it can be confirmed and in accordance with Zhang et al. [25], that in a process of AC reuse over a long period of time it does not significantly alter its textural properties and that the AC can be reused.

4. Conclusion

The results obtained in this study show that in the process of photo-degradation (UV-C/H_2O_2) of DEP, the pH was the variable that most significantly affected the kinetics of degradation. The addition of H_2O_2 produced an increase in the degradation rate of the micro-pollutant, since it promoted an increase in the concentration of HO• radicals. The decomposition rate of DEP in the coupling (UV-C/H_2O_2/AC) was high and the DEP elimination process was the fastest in comparison with other treatments.

Degradation of DEP on the carton is not influenced only by the H_2O_2 concentration, because there was an increase in
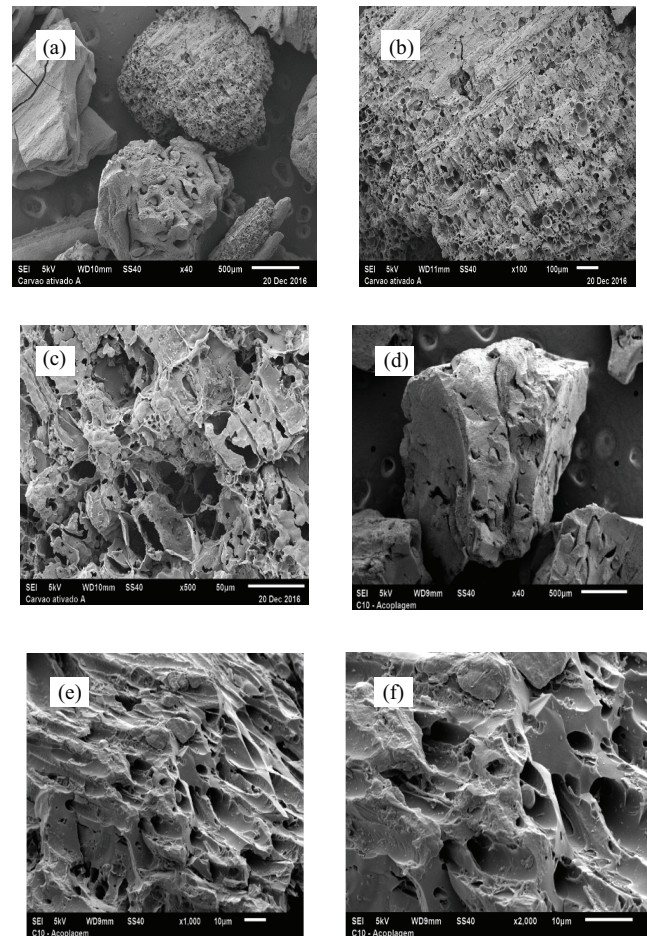

Fig. 8. Pre-kinetic AC SEM images ((a)–(c)), post-kinetic couplings K10 ((d)–(f)).

secondary degradation reactions. The pH variable was, as for the AOP also, the one that caused the greatest significant difference. The presence of AC during DEP degradation increased the coupling efficiency (UV-C/H_2O_2/AC).

The characterization of the AC structure, pre and post the UV-C/H_2O_2/AC process revealed that pre-use and post-use AC MEV images are still smooth. Some carbon particles from the AC prior to use in the treatments are difficult to find in the AC MEV images used. The images also revealed that AC pore structure was not damaged, allowing for an AC reuse process.

Therefore, the coupling proved to be an efficient proposal for the degradation of DEP when compared with the conventional effluent treatment operating conditions. However, it is still necessary to deepen the study of effluent treatment based on matrices with more pollutants.

Symbols

$\delta_{homogeneous}$ — Kinetic contribution of the homogeneous phase, %

$\delta_{heterogeneous}$ — Kinetic contribution of the homogeneous phase, %

$k_{heterogeneous}$ — First-order kinetic constant of the heterogeneous phase, min^{-1}

$k_{homogêneous}$ — First-order kinetic constant of the homogeneous phase, min^{-1}

k_{global} — Global reaction constant in the heterogeneous and homogeneous phase, min^{-1}

$k_{global\ obs}$ — First-order kinetic constant of tert-butanol, min^{-1}

q_e — Amount of solute adsorbed by unit mass of adsorbent, $mg\ g^{-1}$

C_0 — Initial concentrations of the adsorbent in the liquid phase, $mg\ L^{-1}$

C_e — Final concentrations of the adsorbent in the liquid phase, $mg\ L^{-1}$

V — Volume of solution, L

M — Adsorbent mass, g

References

[1] A.R. Ribeiro, O.A.C. Nunes, M.F.R. Pereira, A. Adrián, A.M.T. Silva, An overview on the advanced oxidation processes applied for the treatment of water pollutants defined in the recently launched Directive 2013/39/EU, Environ. Int., 55 (2015) 33–51.

[2] S. Net, R. Sempéré, A. Delmont, A. Paluselli, B. Ouddane, Occurrence, fate, behavior and ecotoxicological state of phthalates in different environmental matrices, Environ. Sci. Technol., 49 (2015) 4019–4035.

[3] K.M. Gani, A.A. Kazmi, Phthalate contamination in aquatic environment a critical review of the process factors that influence their removal in conventional and advanced wastewater treatment, Crit. Rev. Environ. Sci. Technol., 46 (2016) 1402–1449.

[4] H. Wang, H. Li, Q. Song, L. Gao, N. Wang, Adsorption of phthalates on municipal activated sludge, Hind. Publish. Corp. J. Chem., 1 (2017) 1–7.

[5] N.A. Medellin-Castillo, R. Ocampo- Pérez, R. Leyva-Ramos, M. Sánchez-Polo, J. Rivera-Utrilla, J.D. Méndez-Díaz, Removal of diethyl phthalate from water solution by adsorption, photo-oxidation, ozonation and advanced oxidation process (UV/H_2O_2, O_3/H_2O_2 and O_3/activated carbon), Sci. Total Environ., 142 (2013) 25–35.

[6] S. Venkata-Mohan, S. Shailaja, M. Rama Krishna, P.N. Sarma, Adsorptive removal of phthalate ester (diethyl phthalate) from aqueous phase by activated carbon: a kinetic study, J. Hazard. Mater., 146 (2007) 278–282.

[7] J.A. Hoppin, J.W. Brock, B.J. Davis, D.D. Baird, Reproducibility of urinary phthalate metabolites in first morning urine samples, Environ. Health Perspect., 110 (2002) 515–518.

[8] K.M. Shea, Pediatric exposure and potential toxicity of phthalate plasticizers, Pediatrics, 111 (2003) 1467–1474.

[9] G. Latini, Monitoring phthalate exposure in humans, Clin. Chim. Acta, 361 (2005) 20–29.

[10] R. Hauser, A.M. Calafat, Phthalates and human health, Occup. Environ. Med., 62 (2005) 806–818.

[11] G. Latini, A. Del Vecchio, M. Massaro, A. Verrotti, C. De Felice, Phthalate exposure and male infertility, Toxicology, 226 (2006) 90–98.

[12] C.A. Staples, D.R. Peterson, T.F. Parkerton, W.J. Adams, The environmental fate of phthalate esters: a literature review, Chemosphere, 35 (1997) 667.

[13] K. Bekbolet, Z. Çinar, M. Kiliç, C.S. Uyguner, C. Minero, E. Pelizzetti, Photocatalytic oxidation of dinitronaphthalenes: theory and experiment, Chemosphere, 75 (2009) 1008–1014.

[14] Y.-J. Lee, H. Han, S.H. Kim, J.W. Yang, Combination of electrokinetic separation and electrochemical oxidation for acid dye removal from soil, Sep. Sci. Technol., 44 (2009) 2455.

[15] I. Arslan-Alaton, N. Ayten, T. Olmez-Hanci, Photo-Fenton-like treatment of the commercially important H-acid: process optimization by factorial design and effects of photocatalytic treatment on activated sludge inhibition, Appl. Catal. B, 96 (2010) 208–217.

[16] T. Olmez-Hanci, I. Arslan-Alaton, G. Basar, Multivariate analysis of anionic, cationic and nonionic textile surfactant degradation with the H_2O_2/UV-C process by using the capabilities of response surface methodology, J. Hazard. Mater., 185 (2011) 193–203.

[17] A. Karci, I. Arslan-Alaton, T. Olmez-Hanci, M. Bekbolet, Transformation of 2,4-dichlorophenol by H_2O_2/UV-C, Fenton and photo-Fenton processes: oxidation products and toxicity evolution, J. Photochem. Photobiol. A, 230 (2012) 65–73.

[18] I.K. Kalavrouziotis, Wastewater and Biosolids Management, IWA Publishing, UK, 2017, 143 p.

[19] J. Rivera-Utrilla, J. Méndez-Díaz, M. Sánchez-Polo, M.A. Ferro-García, I. Bautista-Toledo, Removal of the surfactant sodium dodecylbenzenesulphonate from water by simultaneous use of ozone and powdered activated carbon: comparison with systems based on O_3 and O_3/H_2O_2, Water Res., 40 (2006) 1717–1725.

[20] Y. Deng, R. Zhao, Advanced oxidation process (AOPs) in wastewater treatment, Water Pollut., 1 (2015) 167–176.

[21] H.F. Stoeckli, Porosity in Carbons: Characterization and Applications, J. Patrick, Ed., Arnold, London, 1995, pp. 67–92.

[22] H.F. Stoeckli, M.V. Lopez-Ramon, D. Hugi-Cleary, A. Guillot, Micropore sizes in activated carbons determined from Dubinin–Radushkevich equation, Carbon, 39 (2001) 1115–1116.

[23] H.P. Boehm, Surface oxides on carbon and their analysis: a critical assessment, Carbon, 40 (2002) 145–149.

[24] J.R. Regalbuto, J.O. Robles, The Engineering of Pt/carbon Catalyst Preparation, University of Illinois, Chicago, 2004.

[25] S. Zhang, Y. Han, L. Wang, Y. Chen, P. Zhang, Treatment of hypersaline industrial wastewater from salicylaldehyde production by heterogeneous catalytic wet peroxide oxidation on commercial activated carbon, Chem. Eng. J., 252 (2014) 141–149.

[26] W. Liu, S.A. Andrews, S.A. Stefan, J.R. Bolton, Optimal methods for quenching H_2O_2 residuals prior to UFC testing, Water Res., 37 (2003) 3697–3703.

[27] T.F. Oliveira, O. Chedeville, B. Cagnon, H. Fauduet, Degradation kinetics of DEP in water by ozone/activated carbon process: influence of pH, Desal. Wat. Treat., 269 (2011) 271–275.

[28] A.M.L. Acosta, Unconventional Treatment Processes for the Degradation of the Antibiotic Sulfadiazine in Aqueous Medium, Doctorate Thesis, Polytechnic School of the University of São Paulo, São Paulo, Brazil, 2016, 113 p.

[29] A.M. Nienow, J.C. Bezares-Cruz, I.C. Poyer, I. Hua, C.T. Jafvert, Hydrogen peroxide-assisted UV photodegradation of lindane, Chemosphere, 72 (2008) 1700–1705.

[30] T.F. Oliveira, O. Chedeville, H. Fauduet, B. Cagnon, Use of ozone/activated carbon coupling to remove diethyl phthalate from water: influence of activated carbon textural and chemical properties, Desalination, 276 (2011) 359–365.

[31] A.L. Ahmad, M.M. Loh, J.A. Aziz, Preparation and characterization of activated carbon from oil palm wood and its evaluation on methylene blue adsorption, Dyes Pigm., 75 (2007) 263–272.

[32] P.H. Ramos, M.C. Guerreiro, E.C. Resende, M. Gonçalves, Production and characterization of activated carbon produced from the black, green, burnt (PVA) defect of the coffee, Quím. Nova, 32 (2009) 1139–1143.

[33] B. Xu, N.-Y. Gao, X.-F. Sun, S.-J. Xia, M. Rui, M.-O. Simonnot, C. Causserand, J.-F. Zhao, Photochemical degradation of diethyl phthalate with UV/H_2O_2, J. Hazard. Mater., 132 (2007) 132–139.

[34] B. Xu, N.-Y. Gao, H. Cheng, S.-J. Xia, M. Rui, D.-D. Zhao, Oxidative degradation of dimethyl phthalate (DMP) by UV/H_2O_2 process, J. Hazard. Mater., 162 (2009) 954–959.

[35] J. Rivera-Utrilla, M. Sánchez-Polo, Ozonation of 1,3,6-naphthalenetrisulphonic acid catalyzed by activated carbon in aqueous phase, Appl. Catal. B, 39 (2002) 319–329.

[36] S. Ledakowicz, M. Gonera, Optimization of oxidants dose for combined chemical and biological treatment of textile wastewater, Water Res., 33 (1999) 2511–2516.

[37] R. Alnaizy, A. Akgerman, Advanced oxidation of phenolic compounds, Adv. Environ. Res., 4 (2000) 233–244.

[38] A.D. Shah, N. Dai, W.A. Mitch, Application of ultraviolet, ozone, and advanced oxidation treatments to washwaters to destroy nitrosamines, nitramines, amines, and aldehydes formed during amine-based carbon capture, Environ. Sci. Technol., 47 (2013) 2799–2808.

[39] J. Brame, M. Long, Q. Li, P. Alvarez, Inhibitory effect of natural organic matter or other background constituents on photocatalytic advanced oxidation process: mechanistic model development and validation, Water Res., 84 (2015) 362–371.

[40] A. Buthiyappan, A. Aziz, A. Raman, W. Daud, W.M. ashri, recent advances and prospects of catalytic advanced oxidation process in treating textile effluents, Rev. Chem. Eng., 32 (2016) 1–47.

[41] H.H. Huang, M.C. Lu, J.N. Chen, C.T. Lee, Catalytic decomposition of hydrogen peroxide and 4-chlorophenol in the presence of modified activated carbons, Chemosphere, 51 (2003) 935–943.

[42] A. Rey, J.A. Zazo, J. A. Casas, A. Bahamonde, J.J. Rodriguez, Influence of the structural and surface characteristics of activated carbon on the catalytic decomposition of hydrogen peroxide, Appl. Catal. A, 402 (2011) 146–155.

[43] L. Dąbek, E. Ozimina, A. Picheta-Oleś, Dye removal efficiency of virgin activated carbon and activated carbon regenerated with Fenton`s reagent, Environ. Protect. Eng., 38 (2012) 5–13.

[44] L. Dąbek, E. Ozimina, A. Picheta-Oleś, Assessing the influence of the presence of heavy metals adsorbed on activated carbon on the efficiency of degradation of phenol using selected oxidizing agents, Soc. Ecol. Chem. Eng. S, 19 (2012) 249–257.

[45] F.J. Beltrán, P. Pocotales, P. Alvarez, A. Oropesa, Diclofenac removal from water with ozone and activated carbon, J. Hazard. Mater., 163 (2009) 768–776.

[46] T.F. Oliveira, B. Cagnon, O. Chedeville, H. Fauduet, Removal of a mix of endocrine disrupter from different natural matrices by ozone/activated carbon coupling process, Desal. Wat. Treat., 52 (2014) 4395–4403.

[47] H. Valdés, A.C. Zaror, Heterogeneous and homogeneous catalytic ozonation of benzothiazole by activated carbon: kinetic approach, Chemosphere, 65 (2006) 1131–1136.

[48] E. De Bel, C. Janssen, S. De Smet, H. Van Langenhove, J. Dewulf, Sonolysis of ciprofloxacin in aqueous solution: influence of operational parameters. Ultrason. Sonochem., 18 (2011) 184–189.

[49] M. Gonçalves, M.C. Guerreiro, M.L. Bianchi, L. C.A. Oliveira, E.I. Pereira, R.M. Dallago, Production of activated carbon from mate grass for the removal of organic contaminants from aqueous medium, Ciên. Agrotecn., 31 (2007) 1386–1391.

[50] B. Cagnon, X. Py, A. Guillot, J.P. Joly, R. Berjoan, Pore modification of pitch-based activated carbon by NaOCl and air oxidation/pyrolysis cycles. Microporous Mesoporous Mater., 80 (2005) 183–193.